

DIRECT SYNTHESIS IRON OXIDE NANOPARTICLES USING RAMIE, LEMON AND DRAGON FRUIT AS GREEN AND LOW COST APPROACH

X. H. Yau¹, W. W. Liu², Z. X. Ooi³ and Y. P. Teoh^{1,*}

¹Department of Chemical Engineering Technology, Faculty of Engineering Technology, University Malaysia Perlis, 01000 Kangar, Perlis, Malaysia

²Institute of Nano Electronic Engineering, Universiti Malaysia Perlis, 01000 Kangar, Perlis, Malaysia

³Department of Chemical Science, Faculty of Science, Universiti Tunku Abdul Rahman, 31900 Kampar, Perak, Malaysia

Published online: 10 November 2017

ABSTRACT

Plant extracts have been used as agent reduction capping to synthesise various nanoparticles due to the process is a low cost, large-scale method and environmental friendly. Herein, iron oxide nanoparticles were synthesized using ramie, lemon and dragon fruit extracts. The characterization results show that all synthesized iron oxide nanoparticles had almost similar diameters, shape and crystalline phases although different of plants extracts were used. Among the plants, ramie has cheapest market price in which the cost production of iron oxide nanoparticles can be reduced significantly.

Keywords: iron oxide nanoparticles; scanning electron microscopy; UV-VIS spectroscopy.

Author Correspondence, e-mail: ypteoh@unimap.edu.my

doi: <http://dx.doi.org/10.4314/jfas.v9i6s.1>



1. INTRODUCTION

Nanotechnology is a modern science which involves the use of the nanoscale materials [1]. Nanotechnology also refer as engineering at molecular level and it is a multi-disciplinary area of applied science and engineering that deals with the manufacture and design of nanoscale components and systems such as computer chips and biosensor [2-3]. Nanoparticles are small in size; thus, it has a larger surface to volume ratio [4]. This characteristic increases the demand of nanoparticles due to their wide application in the field of biomedical, pharmaceutical, electronic, engineering, material science, agricultures and other area [1-4]. For example, iron oxide nanoparticles can be used to remove the arsenic found in water and medical resonance imaging [5].

Iron oxide exist in seven crystalline phase: hematite (α -Fe₂O₃), maghemite (γ -Fe₂O₃), magnetite (Fe₃O₄), wustite (Fe_{1-x}O), β -Fe₂O₃ phase, ϵ -Fe₂O₃ phase and the low temperature rhombohedral structure of magnetite [6]. The hematite, maghemite and magnetite are the common iron oxide that can be produced in the lab. Several physical and chemical methods such as co-precipitation, thermal decomposition, microemulsion, hydrothermal method, sonochemical synthesis have been used to synthesize nanoparticle. But due to the use of costly chemical and production of hazardous by-products, the green method is introduced [7].

Green methods can refer to either the use of microorganisms or the plant extracts. Green method is a cheap, safe and environmental friendly alternative way to synthesise iron oxide nanoparticles. The use of plant extracts has more advantageous in the synthesizing of nanoparticles as compared to the involvement of microorganisms due to the need of maintaining the cell cultures activities and facing difficulty to scale up production rate under non-aseptic environment [8].

There many types of plants have been reported as agent reduction and capping for green synthesis of nanoparticles. To the best of our knowledge, this is considered the first report on the use of ramie, lemon and dragon fruit as agent reduction. Ramie has been used as ingredient in the making cake. In addition, ramie has been applied in medical treatment for diseases such as diuretic and hepatitis B [9]. On the other hand, both lemon and dragon fruit are fruit contain high antioxidant properties and widely consumed by peoples. Lemon is rich in ascorbic acid to fight against the cold or flu [10] whereas dragon fruit is used for collagen

synthesis stimulation, reutilizing and trans-epidermal water loss regulation [11].

In this study, green method is proposed to synthesize iron oxide nanoparticles. The findings from this study could give insight perspective the possibilities toward a scalable and lost cost approach of synthesis of other types of nanoparticles.

2. MATERIALS AND METHODS

2.1. Materials

Iron (II) chloride tetrahydrate ($\text{FeCl}_2 \cdot 4\text{H}_2\text{O}$) and iron (III) chloride hexahydrate ($\text{FeCl}_3 \cdot 6\text{H}_2\text{O}$) were purchased from Aldrich Chemicals and used without further purification. Deionized water was used throughout the experiment.

2.2. Preparation of Plant Extracts

Lemon and dragon fruit were purchased from Kuala Lumpur market, whereas ramie was freshly pluck from the garden of housing area. All plants were rinsed with deionized water to remove the dirt. Lemon and dragon fruit was then cut into smaller pieces with a sterilized scalpel in order to ease the blending process. Then, all plants were blended separately to obtain the plant extracts. The plant extracts were then filtered using pore nylon mesh. The filtrates were then centrifuged at 4000 rpm at 25°C. The supernatant (plant extracts) were collected in a 500 ml schott bottle separately and stored.

2.3. Preparation of Ferric Chloride Solution

4.97 g of iron (II) chloride tetrahydrate ($\text{FeCl}_2 \cdot 4\text{H}_2\text{O}$) and 13.52 g of iron (III) chloride hexahydrate ($\text{FeCl}_3 \cdot 6\text{H}_2\text{O}$) were dissolved in 250 ml of sterilize deionized water in beaker and mixed thoroughly using magnetic stirrer on hot plate.

2.4. Synthesis of Iron Oxide Nanoparticles

250 ml of ferric chloride solution was mixed with 250 ml of plant extracts in a 500 ml beaker. The mixture solution was heated at 50°C under mild stirring by using magnetic stirrer for 2 hours and then left for cool down until room temperature. After cooling, the mixture was undergoing centrifugation process in order to obtain the black precipitate. The mixture solutions were centrifuged at 4000 rpm at 10°C for 10 minutes. The black precipitate were then washed several times by adding deionized water and re-centrifuged to obtain final black samples for further drying at 80°C inside an oven for overnight. A dried powder of iron oxide

nanoparticles was ground with a mortar and pestle. Then, the powder of iron oxide nanoparticles was undergone calcination process in the furnace at 400°C for 8 hours. After calcined, the powder of iron oxide nanoparticles was further grinded by using pestle and mortar to get fine powders. The fine powders were then collected in plastic bag.

2.5.Characterizations

2.5.1. UV-Vis Spectroscopy Analysis

The reduction of ferric chloride was monitored by measuring the absorbance. UV-Vis analysis was conducted using Lambda 35 UV-Vis spectroscopy. The spectra between 200 and 1100nm were scanned to find the absorbance peak.

2.5.2. X-ray Diffraction Analysis

X-ray diffraction (XRD) patterns were recorded with Bruker D2 X-ray diffractometer using CuK α radiation ($\lambda= 0.15406\text{nm}$).

2.5.3. Scanning Electron Microscopy Analysis

JSM-6460LA Scanning electron microscope (SEM) with the magnification power of 10000x was used to examine the morphology of nanoparticles.

2.5.4. Fourier Transform Infrared Spectroscopy Analysis

Fourier transform infrared spectroscopy (FTIR) analysis was employed to determine the possible functional group present in the plant extracts, which responsible for the reduction of iron ions in ferric chloride solution and also acted as the capping stabilization agents. Perkin Elmer FTIR Spectroscopy 100 was used to carry out the analysis in the range of wavelength of 650-4000 cm^{-1} .

3. RESULTS AND DISCUSSION

Three different types of plant extracts have been used for the synthesis of iron oxide nanoparticles Table 1. When the mixture of iron chloride solution (iron (II) chloride tetrahydrate and iron (III) chloridehexahydrate) was added to the plant extracts, the colour changes was observed and shown in Table 2, indicating the formation of iron oxide nanoparticles.

Table 1. Chosen plant for the production of iron oxide nanoparticles

No.	Binomial Name	Common Name	Family Name	Part Taken
1	<i>Boehmerianivea</i>	Ramie	Urticaceae	Leaf
2	<i>Citrus limonum</i>	Lemon	Rutaceae	Fruit
3	<i>Hylocereuscoastaricensis</i>	Dragon fruit	Cactaceae	Fruit

Table 2. Colour changes during the green synthesis of iron oxide nanoparticles solution

No.	Plant Extracts	ColourChange	
		Before	After
1	Ramie	Dark green	Black
2	Lemon	Pale yellow	Pale black
3	Dragon fruit	Magenate	Dark brown

The optical properties of iron oxide nanoparticles were examined by using UV-Vis spectroscopy in the range of 200 to 1100 nm. Fig. 1 shows the absorption coefficient of iron oxide nanoparticles synthesized using ramie, lemon and dragon fruit extract. It can be observed that the absorption values decreased with increasing wavelength from 200-1100 nm. In a more precisely description, the absorption values decreased after the absorbance peak (as mark by arrows in Fig. 1. The presence of absorbance peaks at 233, 232 and 231 nm for ramie, lemon and dragon fruit were not clearly presented. But, a small and flat bump was observed in Fig. 1, which is in agreement with the finding stated by [12]. Small bump occurred as the concentration of reducing agent present in those plant extracts were very low and thus, a little and not obvious excitation of electron in transition states could happened.

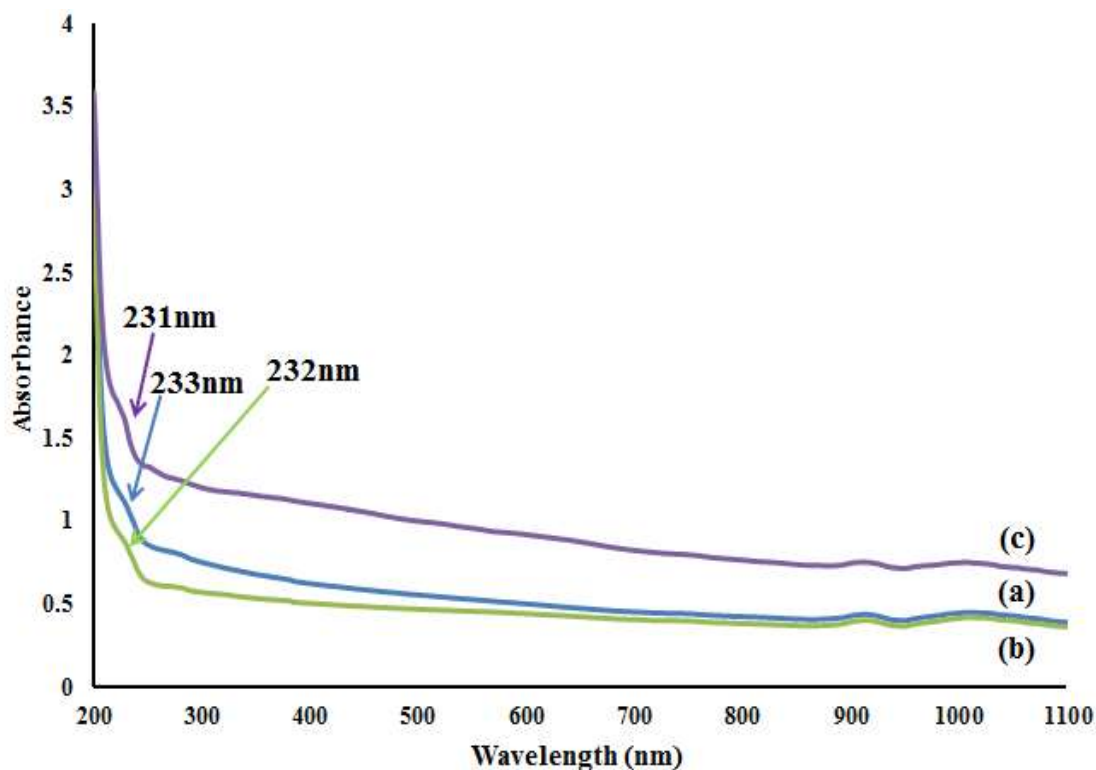


Fig.1. Absorption coefficient of iron oxide nanoparticles produced using (a) ramie, (b) lemon and (c) dragon fruit extracts

XRD is used to characterize the crystal structure of synthesized nanoparticles. Fig. 2 presents the XRD patterns of iron oxide nanoparticles synthesized using various plant extracts (ramie, lemon and dragon fruit). The 2θ values of 24.5° , 33.5° , 36.0° , 41.2° , 49.8° , 54.4° , 62.7° and 64.3° were corresponded to (012), (104), (110), (113), (024), (116), (214) and (300) respectively (Fig. 2a). Fig. 2(b) shows the diffraction peaks of iron oxide nanoparticle synthesized using lemon extract with 2θ values of 24.3° , 33.3° , 35.8° , 41.0° , 49.6° , 54.2° , 62.5° and 64.1° could be well indexed to (012), (104), (110), (113), (024), (116), (214) and (300) respectively. Fig. 2(c) displays the diffraction peaks of iron oxide nanoparticle synthesized using dragon fruit extract with 2θ values of 24.4° , 28.6° , 33.4° , 35.9° , 41.0° , 49.7° , 54.3° , 62.6° and 64.2° were denoted to (012), (220), (104), (110), (113), (024), (116), (214) and (300) respectively. The calcination at 400°C induced the formation of crystalline structure of iron oxide nanoparticles with appearance of several peaks at 24.2° (012), 32.2° (104), 35.7° (110), 40.9° (113), 49.5° (024), 54.1° (116), 62.5° (214) and 64.0° (300) (JCPDF No: 089-2810). Therefore, iron oxide nanoparticles are well matched with the $\beta\text{-Fe}_2\text{O}_3$ phase in

rhombohedral geometry [13-14]. An additional peak was observed for the XRD pattern of iron oxide nanoparticles synthesized using dragon fruit at 2θ values of 28.6° , which is corresponding to (220). This is might be due to the presence of impurities [15]. In contrast, the XRD patterns of iron oxide nanoparticles synthesized using ramie and lemon show no extra diffraction peaks of other phases was detected thus, it indicates the high purity of iron oxide nanoparticles were produced [16].

Besides, the average crystallite size of iron oxide nanoparticles can be calculated by using Debye-Scherrer equation ($d = k\lambda / \beta \cos\theta$ where k is the Scherrer constant (0.9), λ is the wavelength of X-ray (0.15406nm), β is the full width at half maximum and θ is the Bragg angle) [17]. The average crystal size of iron oxide nanoparticles synthesized using ramie, lemon and dragon fruit extracts are 51.30 nm, 51.24nm and 51.26nm. It can be said that all iron oxide nanoparticles synthesized disregard to the type of plant extracts used have the same sizes fall within the range of 40nm to 70nm, which also in agreement with the iron oxide nanoparticles crystallites sizes as stated by [18].

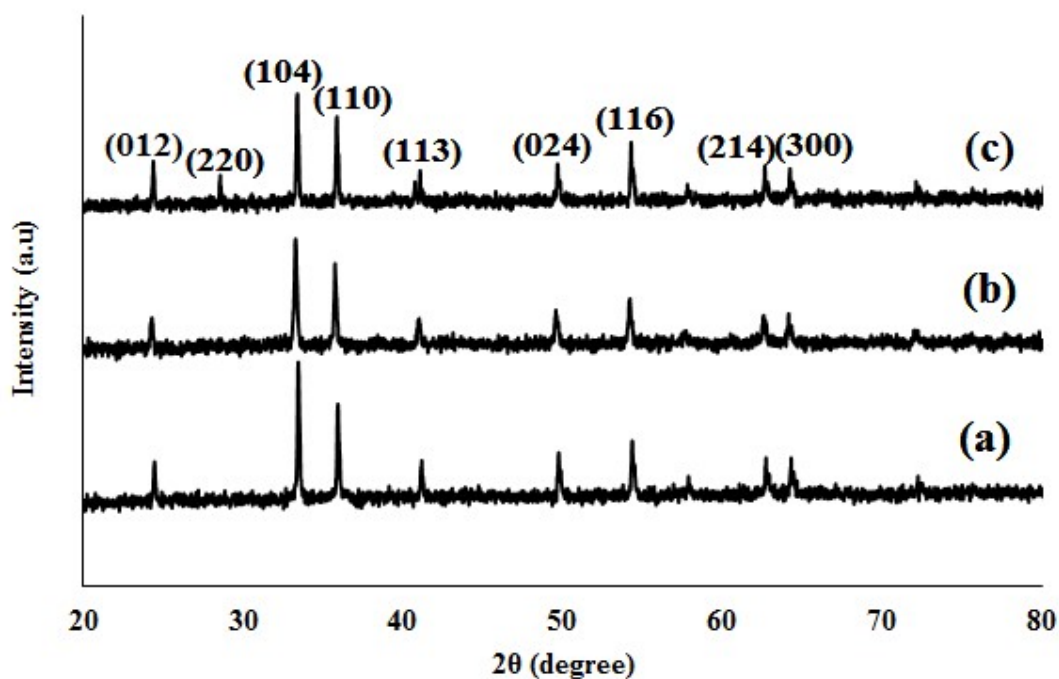


Fig.2. XRD patterns of iron oxide nanoparticles synthesized using (a) ramie, (b) lemon and (c) dragon fruit extracts

The morphology of the synthesized iron oxide particles was investigated by using Scanning Electron Microscopy (SEM). All SEM images are shown in Fig. 3 where irregular spherical

structures were seen. About thirty particles were randomly selected from each image for diameter measurement of the iron oxide particles. Fig. 4 shows the histogram of the size distribution of iron oxide nanoparticles.

Fig. 3(a) and Fig. 4(a) show the SEM image and histogram of size distribution of the iron oxide nanoparticles produced using ramie extracts respectively. The results show that the diameter of synthesized particles had distribution within the range of 100 to 350 nm. The mean diameter of the iron oxide particles synthesized using ramie extracts was about 215.5 nm with a standard deviation of 66.7 nm. The corresponded SEM images show that the particles were observed to have agglomeration form and thus, the bigger diameters of particles were obtained.

Fig. 3(b) and Fig. 4(b) show the morphology image and size distribution of the iron oxide particles produced using lemon extracts in which the particles had diameters distributed within the range of 120 to 480 nm. The mean diameter of the iron oxide particles was approximately 204.8 nm with a standard deviation of 122.7 nm. Large particles with diameter more than 480 nm were seen in the SEM image as shown in Fig. 3(b).

In addition, the iron oxide particles produced using dragon fruit extracts were inspected using SEM (Fig. 3(c)) and their diameters distribution was presented by histogram (Fig. 4(c)). The iron oxide particles demonstrated the diameter in the range 120 to 510 nm. The mean diameter and standard deviation were calculated to be approximately 202.0 and 75.2 nm respectively.

For comparison, the iron oxide particles synthesized using ramie, lemon and dragon fruit extracts demonstrated quite similar diameters (more than 200 nm). The particles produced using ramie show the biggest size of 215.5 nm as compared to others. The agglomeration from small nanoparticles to form big particles was observed in this preparation of crystalline iron oxide particles. The mechanism of agglomeration can be explained using Ostwald ripening [19]. Ostwald ripening is a thermodynamic process which favors the agglomeration of small particles to form large particles. It is because small particles have higher surface energy than large particles which cause them unstable at single small particles. By combining with surrounding particles, the small particles could achieve lower surface energy and the process is continued until the lowest surface energy is obtained [13].

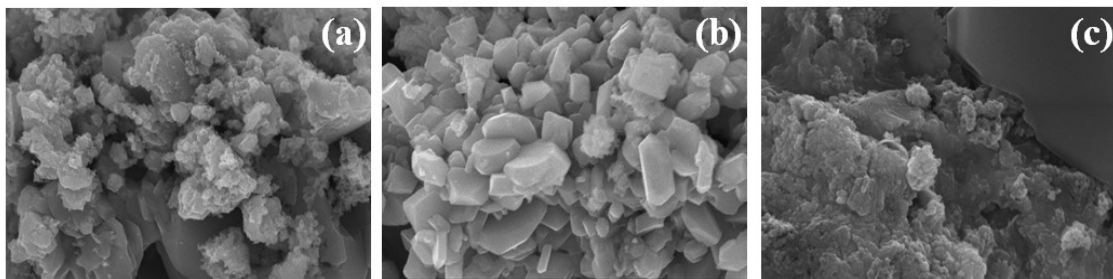
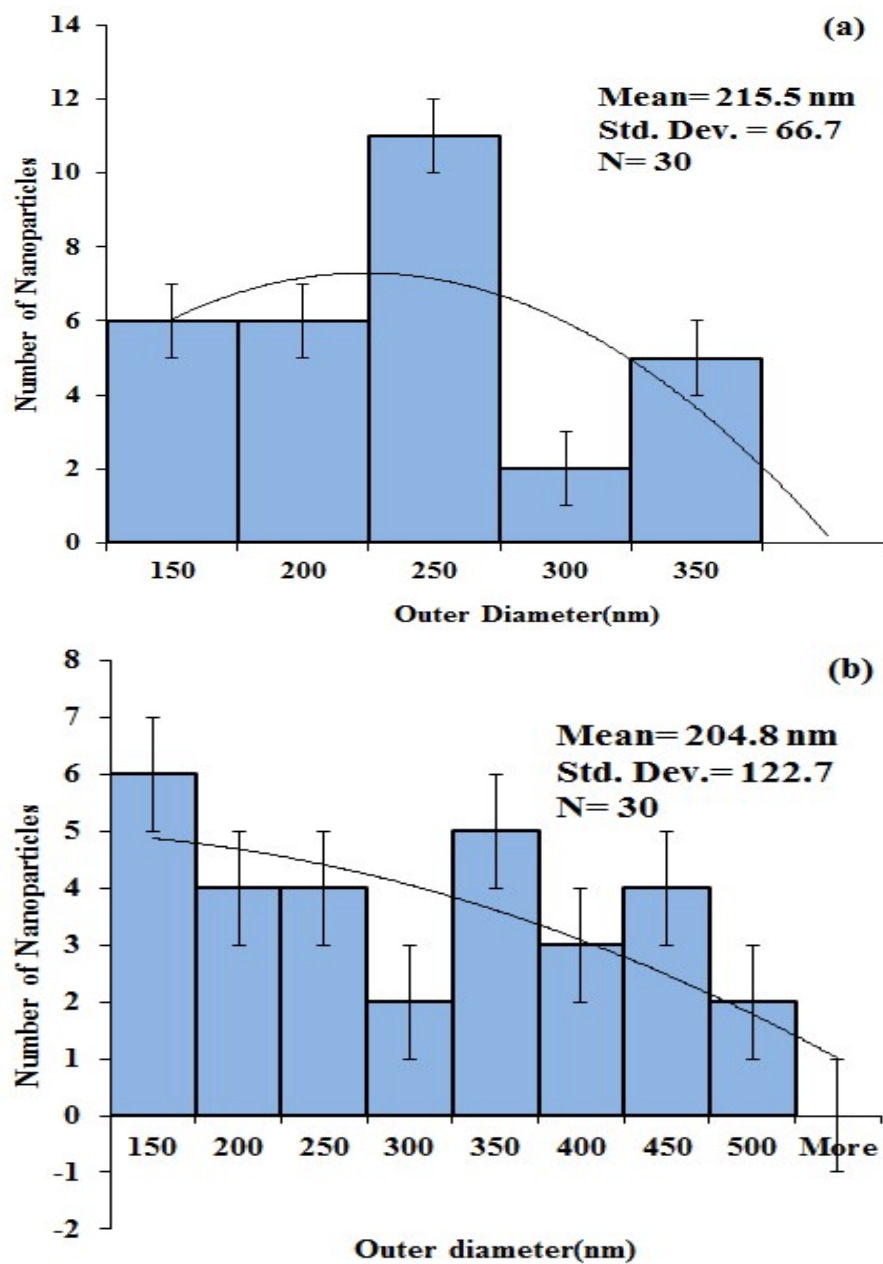


Fig.3. SEM micrographs of iron oxide nanoparticles synthesized using (a) ramie, (b) lemon and (c) dragon fruit extracts



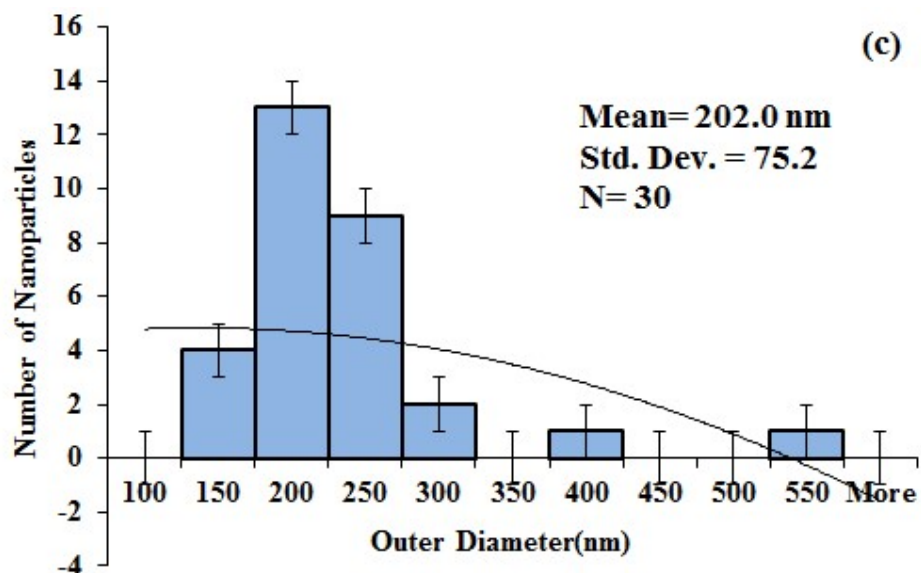


Fig.4. Histogram of size distribution of iron oxide nanoparticles synthesized using (a) ramie, (b) lemon and (c) dragon fruit extracts

Fourier transform infrared spectroscopy (FTIR) analysis is used to identify possible biomolecules from the plant extracts which are responsible for reducing roles Fig. 5.

Fig. 5(a) shows the FTIR spectrum of ramie extracts. The possible functional groups presented by each peak were analyzed and summarized in Table 3. Two absorption peaks at 3368.55 cm^{-1} was attributed to the typical stretching vibration of O-H stretching in both phenol and alcohol groups whereas C=C stretching was identified at 1641.93 cm^{-1} . Additionally, three weak absorption peaks including C=C asymmetric bend stretching at 1498.70 cm^{-1} , C-C stretching at 1406.40 cm^{-1} and C-N stretching vibration at 1290.20 cm^{-1} were observed. The presence of O-H and C=C were believed played as reducing agent for ferric chloride solution as indicated by the change of colour immediately was seen during the reduction.

Table 3. FTIR analysis of ramie extracts

No.	Peak Value (cm ⁻¹)	Functional Groups	Types of Vibration
1	3368.55	Phenols and Alcohol	Hydrogen bonded O-H stretch
2	1641.93	Alkenes	C-C=C symmetric stretch
3	1498.70	Aromatic Rings	C-C=C asymmetric band
4	1406.40	Aromatic Rings	C-C stretch (in rings)
5	1290.20	Aromatic Amines	C-N stretch

Fig. 5(b) shows the FTIR spectrum of lemon extracts. There are about six peaks in the infrared spectrum including two strong intensity peaks (3369.07 cm⁻¹ and 1642.96 cm⁻¹) and four medium intensity peaks (1504.60 cm⁻¹, 1355.70 cm⁻¹, 1227.70 cm⁻¹ and 697.64 cm⁻¹). The possible functional groups were summarized in Table 4. Strong and broad intensity peak of 3369.07 cm⁻¹ indicates the presence of O-H stretching in carboxylic acid. In addition, the appearance of C=O stretching at peak 1642.96 cm⁻¹ further confirms the presence of carboxylic acid in lemon extracts. Thus, the carboxylic acid is the main functional group which acted as the reducing agent in lemon extracts [20].

Table 4. FTIR analysis of lemon extracts

No.	Peak Value (cm ⁻¹)	Functional Groups	Types of Vibration
1	3369.07	Carboxylic acids	Hydrogen bonded O-H stretch
2	1642.96	Carboxylic acid	C=O stretch
3	1504.60	Nitro Groups	N=O stretch
4	1355.70	Nitro Groups	N=O bend
5	1227.70	Aliphatic Amines	C-N stretch
6	697.64	Alkynes	-C≡C-H stretch

Fig. 5(c) shows the FTIR spectrum of dragon fruit extracts. Seven peaks are seen in the infrared spectrum which consist of two high intensity peaks (3369.51 cm⁻¹ and 1643.03 cm⁻¹),

three medium intensity peaks (1498.70 cm^{-1} , 1352.80 cm^{-1} and 1290.20 cm^{-1}) and two low intensity peaks (1129.40 cm^{-1} and 1046.00 cm^{-1}). The possible functional groups were shown in Table 5. Strong and broad peak at 3369.51 cm^{-1} shows the presence of the O-H stretching either from alcohols or phenols group. The aromatic ring of phenol compound was found stretching at 1498.70 cm^{-1} , which indicated their presence in the dragon fruit extracts. Moreover, several peaks appeared at 3369.51 cm^{-1} , 1129.41 cm^{-1} , 1046.00 cm^{-1} and 1290.20 cm^{-1} were assigned to the O-H, C-O and C-N groups respectively which could be the main constituents in the pectin structure. Thus, it is speculated that pectin is the reducing agent from dragon fruit extracts. This is in agreement with the work demonstrated by [21] where pectin was identified as the agent reduction as well.

Table 5. FTIR analysis of dragon fruit extracts

No.	Peak Value (cm^{-1})	Functional Groups	Types of Vibration
1	3369.51	Phenols and Alcohols	Hydrogen bonded O-H stretch
2	1643.03	Alkenes	C-C=C symmetric stretch
3	1498.70	Aromatic Rings	C-C=C asymmetric stretch
4	1352.80	Nitro Compounds	N-O symmetric stretch
5	1290.20	Aromatic Amides	C-N stretch
6	1129.40	Ethers	C-O stretch
7	1046.00	Carboxylic Acids	C-O stretch

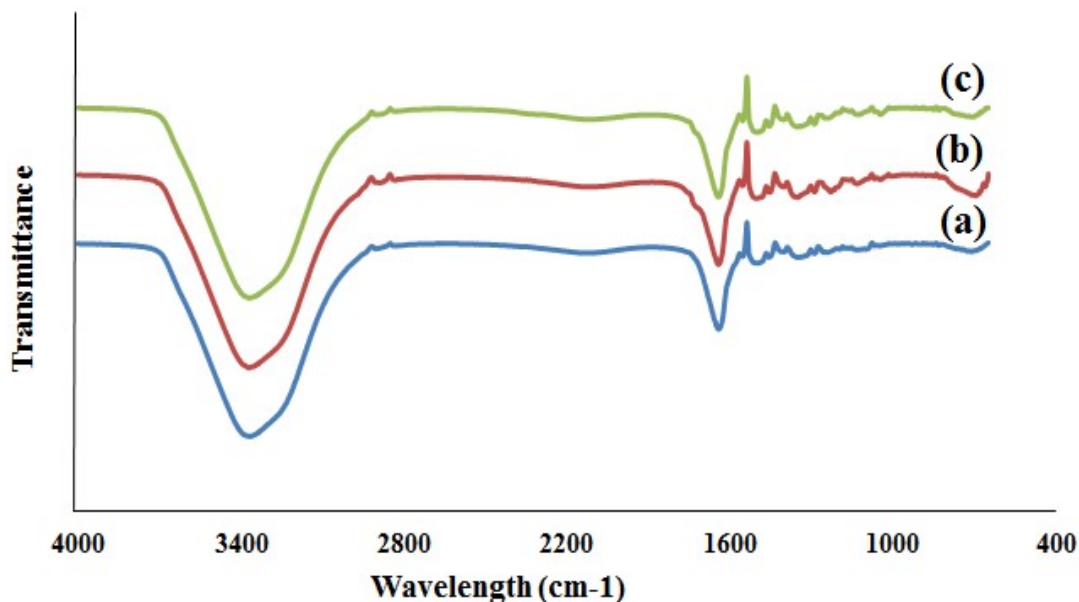


Fig.5.FTIR spectra of (a) ramie, (b) lemon and (c) dragon fruit extracts

4. CONCLUSION

In the present work, we proposed a simple and eco-friendly method to synthesize iron oxide nanoparticles using various plant extracts including ramie, lemon and dragon fruit. The plant extracts were mixed with ferric chloride solution (mixture of iron (II) chloridetetrahydrate and iron (III) chloride hexahydrate) at 50°C under mild stirring condition. A black colour solution was observed in the reaction which is an indication of formation of iron oxide nanoparticles. In the XRD results, it is concludes that the iron oxide nanoparticles with crystallite size of 51 nm were identified as β -Fe₂O₃ and it well matched with JCPDF No: 089-2810. The irregular spherical structure of iron oxide particles was observed and the sized of particles measured within the range of 100 to 510 nm. It is due to the agglomeration of particles was observed clearly in SEM images. The phenolic compounds, carboxylic acids, alkanoids and flavonoids from the plant extracts were recognized as the reducing agent for ferric chloride solution. In overall, this approach is very simple to be conducted and it is cheap and notoxic waste is produced which is environmental friendly.

5. ACKNOWLEDGEMENTS

This work was financially supported by Grant FRGS (Project No.: 9003-00528).

6. REFERENCES

- [1] Priyaa G H, Satyan K B. Biological synthesis of silver nanoparticles using ginger (*Zingiberofficinale*) extract. *Journal of Environmental Nanotechnology*, 2014, 3(4):32-40
- [2] Karkare M. *Nanotechnology: Fundamentals and applications*. New Delhi: I.K. International Publishing House Pvt. Ltd., 2008
- [3] Hosokawa M., Nogi K., Naito M., Yokoyama T. *Nanoparticle technology handbook*. Tokyo: Elsevier, 2007
- [4] Latha N, Gowri M. Bio synthesis and characterisation of Fe₃O₄ nanoparticles using caricaya papaya leaves extract. *International Journal of Scientific Research*, 2014, 3(11):1551-1556
- [5] Siddiqi K S, Rahman A, Tajuddin, Husen A. Biogenic fabrication of iron/iron oxide nanoparticles and their application. *Nanoscale Research Letters*, 2016, 11(1):498-510
- [6] Martinez AI, Garcia-Lobato MA, Perry D L. Study of the properties of iron oxide nanostructures. A. Barranon (Ed.), *Nanotechnology science and technology: New nanotechnology developments*. New York: Nova Science Publishers Inc., 2009, pp. 183-191
- [7] Wu W, He Q, Jiang C. Magnetic iron oxide nanoparticles: synthesis and surface functionalization strategies. *Nanoscale Research Letters*, 2008, 3(11):397-415
- [8] Loo Y Y, Chieng B W, Nisibuch M, Radu S. Synthesis of silver nanoparticles by using tea leaf extract from *Camellia sinensis*. *International Journal of Nanomedicine*, 2012, 7:4263-4267
- [9] Lin C C, Yen M H, Lo T S, Lin J M. Evaluation of the hepatoprotective and antioxidant activity of *Boehmerianivea* var. *nivea* and *Boehmerianivea* var. *tenacissima*. *Journal of Ethnopharmacol*, 1998, 60(1):9-17
- [10] Lal S S, Nayak P L. Green synthesis of gold nanoparticles using various extract of plants and spices. *International Journal of Science Innovations and Discoveries*, 2012, 2(3):325-350
- [11] Perez G R M, Vargas S R, Ortiz H Y D. Wound healing properties of *Hylocereus undatus* on diabetic rats. *Phytotherapy Research*, 2005, 19(8):665-668
- [12] Awwad A M, Salem N M. A green and facile approach for synthesis of magnetite

nanoparticles. *Nanoscience and Nanotechnology*, 2012, 2(6):208-213

[13] Balamurugan M, Saravanan S, Soga T. Synthesis of iron oxide nanoparticles by using *Eucalyptus globulus* plant extract. *e-Journal of Surface Science and Nanotechnology*, 2014, 12(8):363-367

[14] Rahman M M, Khan S B, Jamal A, Faisal M, Aisiri M. Iron oxide nanoparticles. M. M. Rahman (Ed.), *Nanomaterials*. Rijeka: InTech, 2011, pp. 43-66

[15] Awwad A M, Albiss B A, Salem N M. Antibacterial activity of synthesized copper oxide nanoparticles using *Malvasylvestris* leaf extract. *SMU Medical Journal*, 2015, 2(1):91-98

[16] Yew Y P, Shameli K, Miyake M, Kuwano N, Khairudin N B A, Mohamad SE, Lee K X. Green synthesis of magnetite (Fe_3O_4) nanoparticles using seaweed (*Kappaphycus alvarezii*) extract. *Nanoscale Research Letters*, 2016, 11(1):276-282

[17] Mahdavi M, Namvar F, Ahmad M B, Mohamad R. Green biosynthesis and characterization of magnetic iron oxide (Fe_3O_4) nanoparticles using seaweed (*Sargassum muticum*) aqueous extract. *Molecules*, 2013, 18(6):5954-5964

[18] Ahmmad B, Leonard K, Shariful Islam M, Kurawaki J, Muruganandham M, Ohkubo T, Kuroda Y. Green synthesis of mesoporous hematite ($\alpha\text{-Fe}_2\text{O}_3$) nanoparticle and their photocatalytic activity. *Advanced Powder Technology*, 2013, 24(1):160-167

[19] Voorhees P W. The theory of Ostwald ripening. *Journal of Statistical Physics*, 1985, 38(1):231-252

[20] Prathna T C, Chandrasekaran N, Raichur A M, Mukherjee A. Biomimetic synthesis of silver nanoparticles by *Citrus limon* (lemon) aqueous extract and theoretical prediction of particle size. *Colloids and Surfaces B: Biointerfaces*, 2010, 82(1):152-159

[21] Zahran M K, Ahmed H B, Rafie M H. Facile size-regulated synthesis of silver nanoparticles using pectin. *Carbohydrate Polymers*, 2014, 111:971-978

How to cite this article:

Yau X H, Teoh Y P, Liu W W and Ooi Z X. Direct synthesis iron oxide nanoparticles using ramie, lemon and dragon fruit as green and low cost approach. *J. Fundam. Appl. Sci.*, 2017, 9(6S), 1-15.